

## FREE-SPACE INTEGRATED OPTICS REALIZED BY SURFACE-MICROMACHINING

M. C. WU, L. Y. LIN, S. S. LEE, and C. R. KING

*Electrical Engineering Department, University of California at Los Angeles,  
405 Hilgard Avenue, Los Angeles, CA 90095-1594, USA*

A surface-micromachined free-space micro-optical bench (FS-MOB) technology has been proposed to monolithically integrate micro-optical elements, optomechanical structures, micropositioners, and microactuators on the same substrate. Novel three-dimensional micro-optical elements have been fabricated by surface-micromachining techniques. The optical axes of these optical elements are parallel to the substrate, which enables the entire free-space optical system to be integrated on a single substrate. Micro-scale Fresnel lenses, refractive microlenses, mirrors, beam-splitters, gratings, and precision optical mounts have been successfully fabricated and characterized. Integration of micro-optical elements with translation or rotation stages provides on-chip optical alignment or optomechanical switching. This new free-space micro-optical bench technology could significantly reduce the size, weight, and cost of most optical systems, and could have a significant impact on optical switching, optical sensing and optical data storage systems as well as packaging of optoelectronic components.

### 1. Introduction

Integrating entire optical systems on a single semiconductor chip has been the goal of many researchers since Stewart Miller proposed the concept of integrated optics in 1969.<sup>1</sup> Integrated optics offers many advantages over conventional systems, including small size, light weight, higher functionality, and elimination of intermediate packaging and assembly steps. Since packaging and assembly accounts for a large part of the cost of optical modules, integration could lead to a significant reduction in the system cost. Higher performance can also be achieved by better matching the interface between optical elements and reducing the coupling loss. In the past two decades, there has been significant progress in guided-wave integrated optics which is now known as photonic integrated circuits (PIC).<sup>2</sup> The PIC is particularly suitable for integrating active optoelectronic devices such as semiconductor lasers, modulators, and photodetectors with passive waveguides. It has applications in, for example, high performance transmitters and receivers for optical communications networks.

Free-space integrated optics in which photons propagate in space between optical elements, on the other hand, has many applications in display, optical sensing, printing, optical data storage, optical interconnect and signal processing. To date, most of the free-space optical systems are not integrated because the

optomechanical structures and micropositioning stages are not compatible with conventional integrated optics techniques. Recently, there has been growing interest in applying micromachining techniques to create new optomechanical devices as well as to integrate many free-space optical elements on the same substrate.<sup>3,4</sup> Micromachining offers an inexpensive and reproducible batch processing technique to fabricate micro-optical components and microactuators on the same substrate. It also enables wafer-scale integration of the micro-optical systems.

Most of the previous efforts in micromachined optics have focused on the creation of new optomechanical devices. For example, scanning micromirrors,<sup>5</sup> digital micromirrors for digital light processing (display and printing),<sup>6,7</sup> deformable grating light valves for display applications,<sup>8</sup> microfabricated optical choppers,<sup>9</sup> microscanners with gratings and micromotor,<sup>10</sup> and tunable optical filters.<sup>11–15</sup> Micromechanical structures have also been combined with active optoelectronic devices to form tunable edge-emitting lasers<sup>16</sup> and vertical-cavity surface-emitting lasers.<sup>17,18</sup> Most of these components are designed to have surface-normal optical access because the optical elements are confined to the plane of the substrate. They are suitable for forming large two-dimensional arrays. However, it is not possible to cascade two or more optical elements along the optical axes without the help of external optical elements. As a result, they are not suitable for wafer-scale integration of entire optical systems.

Integrating free-space optical systems on a chip is challenging for several reasons: First, it requires integrable free-space optical elements. Although systems composed of separately produced elements installed in alignment holes etched on silicon substrates have been demonstrated in conventional silicon optical benches and waferboards,<sup>19,20</sup> monolithic, batch-fabricated free-space optical elements are preferred. Second, because cascading of multiple-elements requires that the system's optical axis be parallel to the substrate, and because free-space beams are usually expanded to diameters of several hundred micrometers, very tall three-dimensional optical elements are needed. Such components are not compatible with conventional planar fabrication techniques of Si processing. Third, on-chip optical alignment capability must be available. Integrated micropositioning stages are needed for optical alignment, switching, or scanning. Micromachined microactuators such as micromotors, comb-drives, micro-vibromotors, scratch actuators, and thermal actuators are ideal for moving the micro-optical elements.<sup>21–25</sup>

Previously, using a surface-micromachined microhinge technology,<sup>26</sup> we have proposed and demonstrated a *free-space micro-optical bench* (FS-MOB) technology in which three-dimensional free-space micro-optical elements and movable micromechanical structures are fabricated on the same wafer using batch processing techniques.<sup>27,28</sup> Both diffractive and refractive optical elements can be incorporated in FS-MOB. Out-of-plane, three-dimensional micro-Fresnel lenses with diameters as large as 650  $\mu\text{m}$  have been demonstrated.<sup>29,30</sup> Similar techniques have also been applied to fabricate out-of-plane refractive microlenses,<sup>31</sup> micro-gratings,<sup>32</sup> micromirrors,<sup>30,33</sup> etalons,<sup>14,34</sup> and other optical elements. More significantly, these

micro-optical elements can be integrated with micropositioners and microactuators using the same surface-micromachining techniques. A sliding-tilting micro-mirror for coupling lasers to optical fibers,<sup>35</sup> a three-dimensional corner cube reflector with torsion modulators,<sup>36</sup> a  $2 \times 2$  free-space fiber optic switch,<sup>37</sup> a single-chip optical disk pickup head,<sup>38</sup> and a microactuated scanner<sup>39</sup> have also been demonstrated. Three-dimensional alignment structures have also been developed to incorporate active optoelectronic devices.<sup>40,41</sup>

In this paper, we present the design, fabrication processes, and measurement results of various integrable three-dimensional micro-optical elements. Their applications in various micro-optical systems will also be described.

## 2. Design and Fabrication

The concept of the FS-MOB is illustrated in Fig. 1. As in conventional systems constructed on laboratory optical tables, the FS-MOB includes passive optical elements (lenses, gratings, beamsplitters, filters, etc.), micropositioners (translation and rotation stages), microactuators, and active optoelectronic components (lasers, photodetectors). Unlike conventional systems, however, the FS-MOBs are micron-scaled and batch-fabricated on a Si substrate. Because the micro-optical elements on the FS-MOB are precisely placed by photolithography, they can be pre-aligned during the photomask layout. To compensate for fabrication tolerances, fine optical alignment is performed with on-chip micropositioners and microactuators. The FS-MOB has many advantages: Most of the expensive assembly and packaging processes of individual optical components can be eliminated. The system cost, size, and weight are significantly reduced.

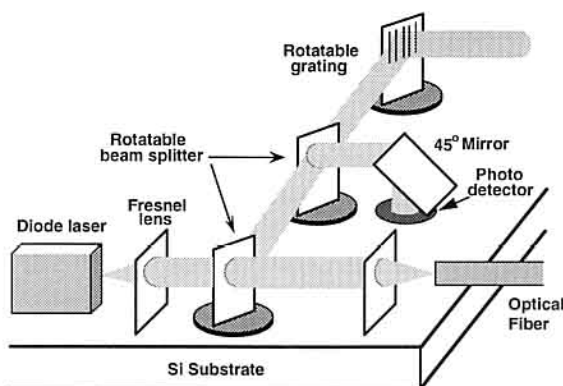


Fig. 1. Schematic drawing illustrating the concept of free-space micro-optical bench (FS-MOB).

The schematic diagram of a three-dimensional micro-Fresnel lens before assembly is shown in Fig. 2. The micro-Fresnel lens is held by the microhinges. The microhinge technology allows out-of-plane optical elements to be made by conventional planar microfabrication techniques, then folded into three-dimensional

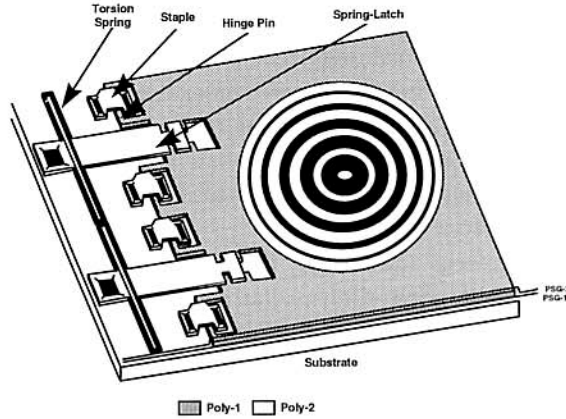


Fig. 2. Schematic diagram of the micro-Fresnel lens before assembly.

structures. Both the micro-optical elements and the microhinges can be made by standard three-polysilicon-layer surface-micromachining processes such as those offered by MCNC.<sup>42</sup> The fabrication processes are described as follows: First, a 0.5  $\mu\text{m}$ -thick silicon nitride layer is deposited on an *n*-doped Si substrate as an insulating layer. Then a 0.5  $\mu\text{m}$ -thick polysilicon layer (poly-0) is deposited for electrical interconnection of microactuators. Next, a 2  $\mu\text{m}$ -thick phosphosilicate glass (PSG-1) is deposited on the silicon substrate as the sacrificial material. It is followed by the deposition of a 2  $\mu\text{m}$ -thick polysilicon layer (poly-1) on which the micro-optic patterns such as Fresnel lenses, mirrors, beam-splitters and gratings are defined by photolithography and chlorine-based dry etching. The hinge pins holding these three-dimensional structures are also defined on this layer. Following the deposition and patterning of poly-1, another layer of sacrificial material (PSG-2) of 0.75  $\mu\text{m}$  thickness is deposited. The supporting structures such as staples and spring latches are defined on the second polysilicon (poly-2) layer. The base of the staples and torsion springs are fixed on the Si substrate by opening contact holes through both PSG-2 and PSG-1 before the deposition of the poly-2 layer. The poly-2 structures can also be contacted with poly-1 by etching contact holes through PSG-2 only, as required in the rotatable mirrors and gratings which will be described later. The micro-optics plates are released from the substrate by selectively removing the PSG material using hydrofluoric acid after fabrication. After the release etching, the polysilicon plates with micro-optic patterns are free to rotate out of the substrate plane. The angles between the plates and the substrate are coarsely defined by the length of the spring latches. Various types of coatings are applied to the three-dimensional optic plates. For example, a thick layer of gold is coated to improve the reflectivity of micromirrors, or to block light transmission through the dark zones of Fresnel zone plates. On the other hand, a thin layer of gold is used for partially transmitting mirrors or beam-splitters. Dielectric coating can also be employed. The coating could be done either before or after the assembly.

### 3. Results and Discussion

#### 3.1. Diffractive optical elements

A three-dimensional micro-Fresnel lens has been fabricated and characterized. The Fresnel zone pattern is defined on the first polysilicon layer by photolithography and dry etching. Figure 3 shows the scanning electron micrograph (SEM) of the micro-Fresnel lens. The lens has a diameter of  $280\ \mu\text{m}$ , and an optical axis of  $254\ \mu\text{m}$  above the silicon surface. Fresnel lenses with diameters as large as  $650\ \mu\text{m}$  and optic plates as tall as  $1.4\ \text{mm}$  have been realized by similar fabrication techniques. The lens angle is precisely fixed by a “lens-mount” consisting of two hinged plates made by the same fabrication processes but folded orthogonally to the lens. The  $2\ \mu\text{m}$ -wide groove at the end of the V-shaped opening firmly locks the position of the lens. Tilting angles smaller than  $0.5^\circ$  can be achieved. The lens mounts also improve the mechanical strength and stability of the lens plate.

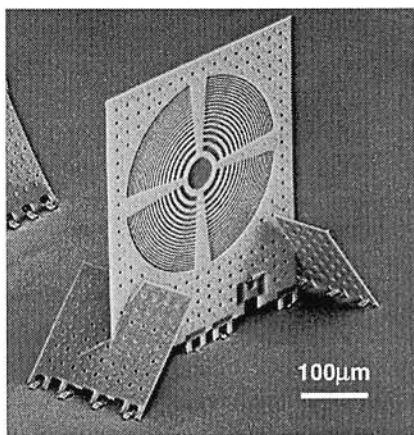


Fig. 3. The SEM micrograph of the micro-Fresnel lens with diameter of  $280\ \mu\text{m}$ .

The lens exhibits very good optical performance. The output beam from a single mode fiber is successfully collimated by the lens. Figure 4 shows the collimated beam profile. Very good agreement with a standard Gaussian shape is obtained (95% fit). Figure 5 compares the divergence angles of the optical beams with and without the collimating lens. The intensity full-width-at-half-maximum (FWHM) angle is reduced from  $5.0^\circ$  to  $0.33^\circ$ . The diffraction efficiency of the micro-Fresnel lens was measured to be 8.6% using the method described by Rastani *et al.*<sup>43</sup> This is in agreement with the theoretical limit of binary-amplitude Fresnel zone plates. A higher theoretical diffraction efficiency of 41% can be achieved by using a binary-phase Fresnel lens. Efficiencies greater than 80% can be achieved by multi-level Fresnel lenses at the expense of more complicated fabrication processes. Another alternative method for achieving high efficiency is to use a refractive lens, as described in the next section.

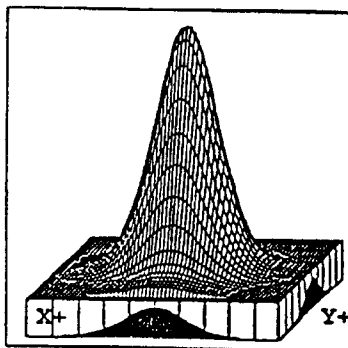


Fig. 4. Profile of the optical beam collimated by the micro-Fresnel lens.

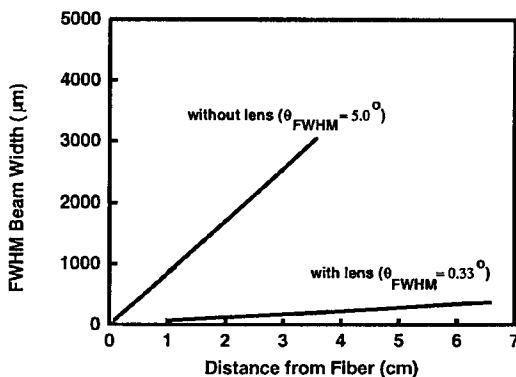


Fig. 5. The FWHM width of the optical beams emitted from a single mode fiber with and without passing through the micro-Fresnel lens.

### 3.2. Refractive microlenses

Refractive optical elements can also be made on FS-MOB by combining the surface-micromachining processes with micro-optics fabrication techniques. The reflow technique has been used to produce high performance microlenses in photoresist and polyimide. By depositing the photoresist on a hinged polysilicon plate, the microlens can be made vertical to the substrate by rotating the supporting polysilicon plate after the reflow processes. Figure 6 shows the schematic drawing and the SEM micrograph of an out-of-plane refractive microlens. The lens is realized by heating a 20  $\mu\text{m}$ -thick AZ 4620 photoresist cylinder to 200°C, causing the photoresist to reflow into a spherical shape, as shown in Fig. 7. The lens is 30  $\mu\text{m}$  thick at the center, and the maximum deviation from a spherical curvature is less than 0.5  $\mu\text{m}$  to within 5  $\mu\text{m}$  of the edges. The resulting lens has a diameter of 300  $\mu\text{m}$  and a focal length of 670  $\mu\text{m}$ . Refractive microlenses with F-numbers ranging from 1 to 5 and diameters from 30  $\mu\text{m}$  to over 500  $\mu\text{m}$  can be made by this technique. The optical loss through the microlens is measured to be 0.7 dB at a wavelength of 632 nm. Lower

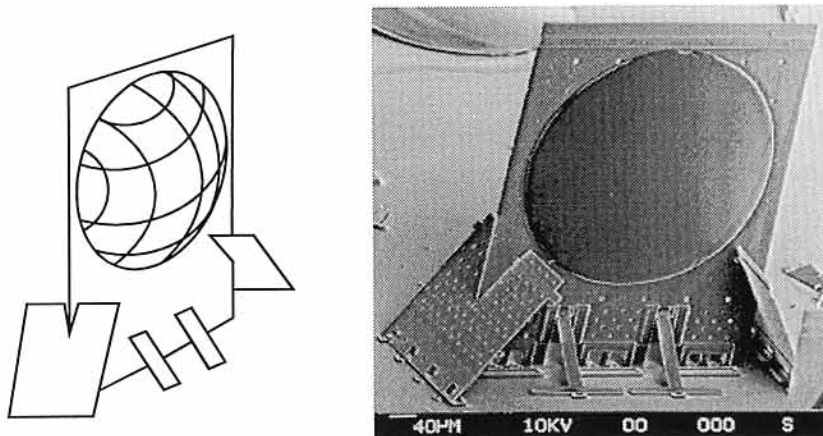


Fig. 6. The schematic drawing and SEM micrograph of the out-of-plane refractive microlens.

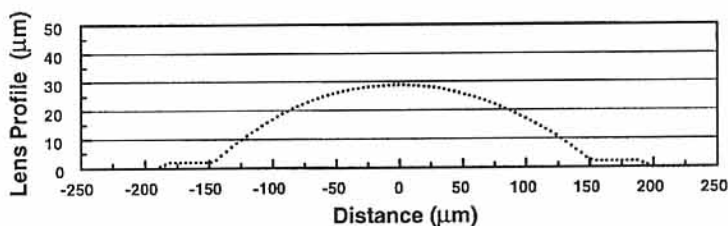


Fig. 7. The surface profile of the refractive microlens.

loss could be expected at longer wavelengths. The optical axis of the microlens is fixed to the same height as the rest of the FS-MOB by photolithography. Very good optical performance has been achieved. Compared with the micro-Fresnel lens, the refractive microlens offers higher efficiency and a wavelength-independent focal length.

### 3.3. Integration with micropositioners and microactuators

The microlenses and other out-of-plane micro-optical elements can be integrated with translation and rotation stages by attaching the microhinges to a moveable polysilicon plate. This can be realized by the same surface-micromachining processes as described earlier. The linear translation stages are realized by confining a released poly-1 plate by a pair of rails made on poly-2 layers. The rotation stages consist of structures similar to those in micromotors.<sup>21</sup> The micro-optics plate is now defined on the second polysilicon layer, and connected to the microhinges defined on poly-1 through via holes. The bases of the spring-latches and staples (poly-2) are now connected to a moveable plate on poly-1 instead of the substrate. Figure 8 shows the SEM micrograph of a three-dimensional micro-grating integrated with

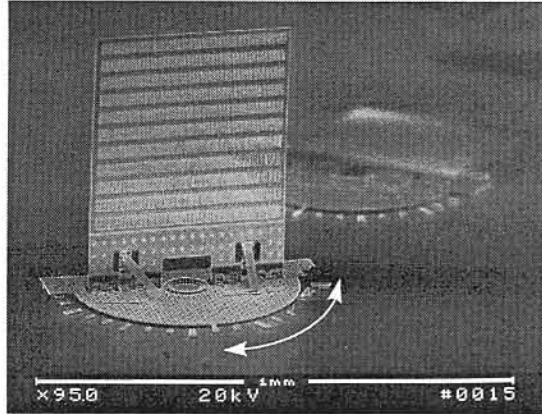


Fig. 8. The SEM micrograph of the micro-grating integrated on a rotation stage.

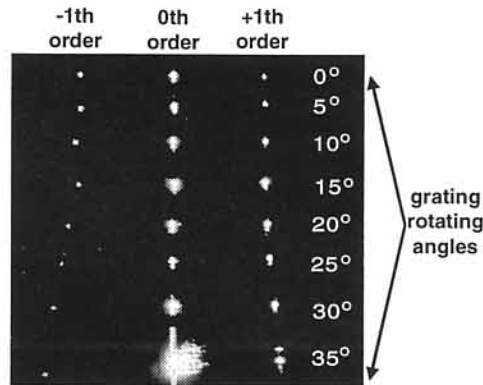


Fig. 9. The diffraction patterns of a micro-grating at various angles of the rotation stage.

a rotation stage. The rotation stage in the SEM has been rotated by  $20^\circ$ . The grating diffraction patterns at various rotation angles (from  $-35^\circ$  to  $+35^\circ$ ) have been successfully observed, as shown in Fig. 9.

### 3.4. Tunable optical filters

Tunable Fabry-Pérot (FP) filters that can be integrated with other micro-optical components or fiber alignment V-groove structures on FS-MOB are very useful for wavelength-division-multiplexed (WDM) optical communications, optical sensing, and spectral analysis applications. Both parallel-plate FP filters and solid FP etalons can be formed by the FS-MOB technique. Figure 10 shows the schematic drawing and the SEM micrograph of a solid etalon. The filter is formed by applying three pairs of Si/SiO<sub>2</sub> dielectric layers as mirrors on both sides of a  $1.6\ \mu\text{m}$ -thick



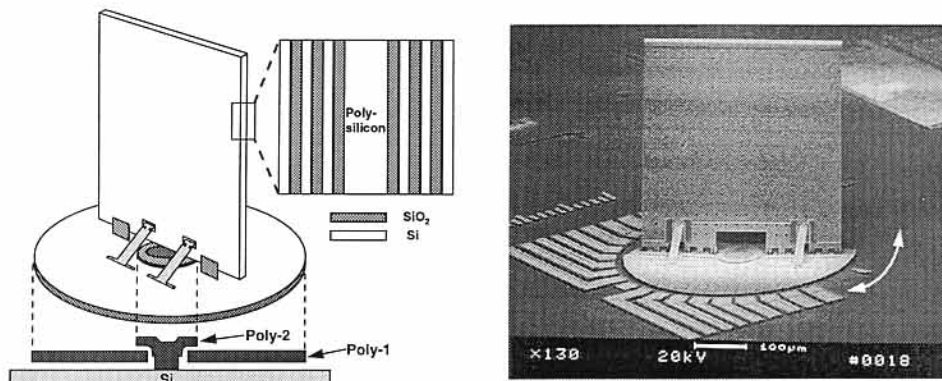


Fig. 10. The schematic and SEM of the tunable solid Fabry-Pérot etalon.

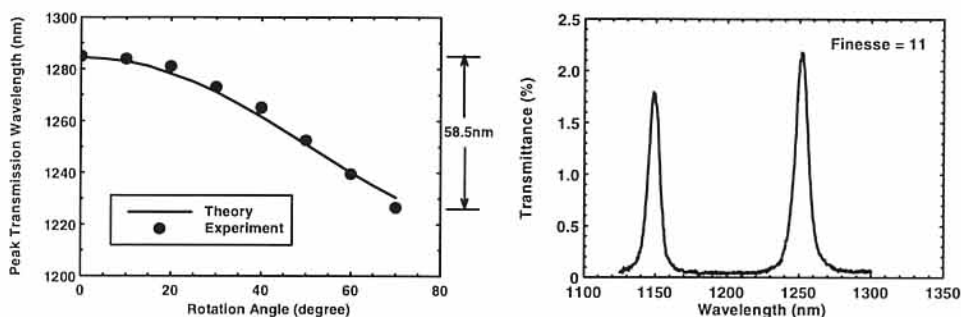


Fig. 11. The wavelength tuning range and the transmission spectrum of the tunable filter.

vertical polysilicon plate. The etalon is built on a rotation stage for angle tuning of the transmission wavelength. Figure 11 shows the transmission wavelength versus the angle of the etalon graph. A broad tuning range of 58.5 nm is obtained. The tuning characteristics agree very well with theory. The transmission spectrum of the etalon at an angle of  $50^\circ$  is also shown in Fig. 11. The finesse of the etalon is measured to be 11, currently limited by the scattering loss at the surface of the polysilicon plate. The finesse can be improved by employing parallel plate FP etalons and smoothening the surface of the polysilicon plate by chemical mechanical polishing.

### 3.5. Free-space fiber optic switches

The FS-MOB technology is ideal for implementing optomechanical switches. The optomechanical switches have the advantages of very low insertion loss and high isolation. One of the most widely used optomechanical switches in local area fiber-optic networks is the FDDI (fiber data distribution interface) optical bypass switch. This switch allows the network to bypass the failed computer node and maintain

the integrity of the network operation. Previously, bulk micromachining on a Si substrate had been employed to implement the FDDI switch.<sup>19</sup> However, it still requires substantial assembly.

We have used the FS-MOB technology to realize a  $2 \times 2$  free-space fiber optic switch. Figure 12 shows the schematic diagram and the SEM micrograph of the switch. It consists of a moveable micromirror, two input and two output fibers arranged in a cross configuration. The switch operates in reflection mode when the mirror is moved between the fibers, and in the transmission mode when the mirror is moved out. The out-of-plane micromirror is made by the same surface-micromachining processes as described earlier. It is integrated with a linear translation stage with travel distance larger than the diameter of the fiber core ( $62.5 \mu\text{m}$ ). To reduce the insertion and diffraction loss, the tips of the optical fibers have been made into the shape of a lens. The insertion loss has been measured to be 1.3 dB for the transmission state, and 1.9 dB for the reflection state. These losses include the Fresnel loss of 0.34 dB, which can be eliminated by anti-reflection coating. By further optimizing the fiber lenses, an insertion loss of below 1 dB is achievable. The linear translation stage can be driven by microactuators with long travel ranges such as the thermal actuators, linear vibromotors or scratch actuators.

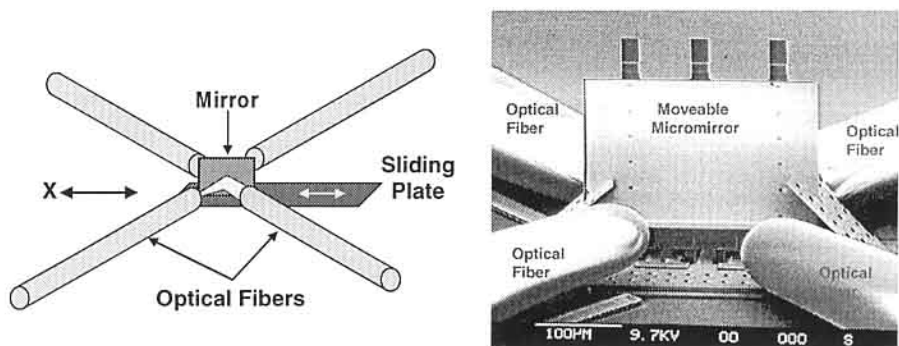


Fig. 12. The schematic and SEM of the free-space fiber-optic switch.

### 3.6. Self-aligned supporting structures for hybrid-integrated optoelectronic components

Most of the micro-optical elements in the FS-MOB are monolithically integrated by the surface-micromachining processes and can be pre-aligned during the design and fabrication process. However, some active optoelectronic components such as lasers cannot be fabricated by this process, and hybrid integration is thus necessary to realize the free-space optical system on a single chip. Though the optoelectronic devices cannot be directly aligned, it is possible to design some novel three-dimensional supporting structures that can be pre-aligned with the rest of the FS-MOB.

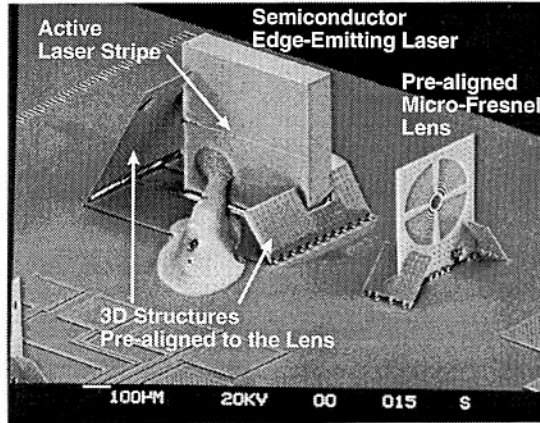


Fig. 13. The SEM micrograph of the semiconductor laser/microlens module. The semiconductor laser has been pre-aligned with the lens by the three-dimensional alignment plates.

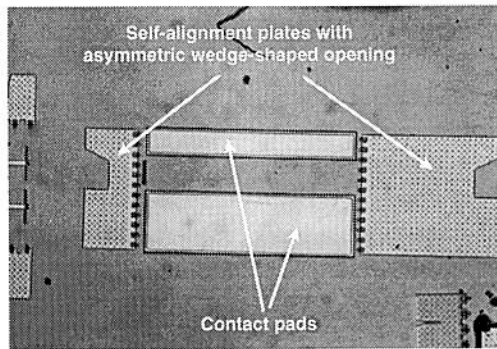


Fig. 14. Top view photograph of the three-dimensional alignment plates before assembly. The flat edges of the openings have been pre-aligned with the center of the microlens.

Figure 13 shows the SEM micrograph of a semiconductor edge-emitting laser pre-aligned with a micro-Fresnel lens. The edge-emitting laser, side-mounted to match the height of the optical axis of the FS-MOB ( $254\ \mu\text{m}$  above the Si surface), is laterally aligned with the micro-Fresnel lens by a pair of three-dimensional plates with an asymmetric opening at the top. Figure 14 is the top view photograph of the self-alignment structures before they are assembled. The flat edge of the opening is pre-aligned with the center of the Fresnel lens and holds the front (emitting) side of the laser. When the alignment plates are assembled and pushed down onto the laser, the oblique rear edges push the laser forward such that the front surface of the device contacts the flat edges. This design allows us to accommodate diode lasers with substrate thicknesses varying from 100 to  $140\ \mu\text{m}$ . Conductive silver epoxy is applied between the laser and the contact pads providing the electrical

contact in this initial demonstration. Potentially, the epoxy could be replaced by other three-dimensional micromechanical structures.

The optical performance of the integrated edge-emitting laser/micro-Fresnel lens set has been characterized. A diode laser with  $1.3\ \mu\text{m}$  wavelength is positioned at the focal point of a Fresnel lens with a  $500\ \mu\text{m}$  focal length. The light emitted by the laser is collimated by the Fresnel lens. The collimated beam profile agrees very well with the Gaussian shape. The FWHM angles of the laser have been reduced from  $18^\circ \times 40^\circ$  to  $0.38^\circ \times 0.9^\circ$ . The elliptical shape is due to the intrinsically asymmetric beam profile which is characteristic of semiconductor edge-emitting lasers.

A similar design can be employed to incorporate vertical cavity surface-emitting lasers (VCSEL). VCSELs have many unique advantages such as low threshold current, circular far-field pattern, narrow beam divergence, and the ability to form two-dimensional arrays. They are very useful for optical interconnects and many other applications. The schematic diagram and the SEM micrograph of a vertical three-dimensional micro-Fresnel lens array and a VCSEL array are shown in Fig. 15. The  $8 \times 1$  VCSEL array is  $2\ \text{mm}$  wide,  $350\ \mu\text{m}$  high, and  $125\ \mu\text{m}$  thick, and the spacing between individual VCSELs is  $250\ \mu\text{m}$ . The VCSEL array is also side-mounted so that the emitting spots match the optical axis of the lens array. Again, the tall three-dimensional alignment structures are built at the same time as the micro-Fresnel lens array. The alignment structures push the VCSEL array forward so that the front surface (emitting side) of the VCSEL array is aligned with the focal plane of the lens array. Individual modulation of the collimated output beam from the VCSEL/lens module has been demonstrated.

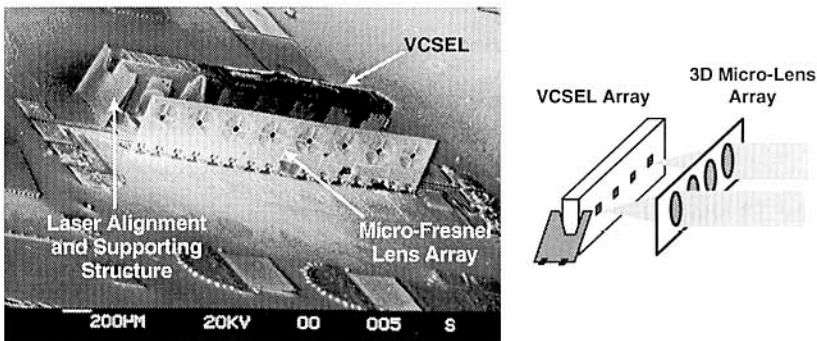


Fig. 15. An  $8 \times 1$  array of vertical cavity surface-emitting lasers aligned with an  $8 \times 1$  array of micro-Fresnel lenses.

For high power operation, it may not be desirable to mount the semiconductor laser on the side because of heat sinking considerations. Upright mounting or junction side down mounting provides better heat sinking. In both cases, direct matching of the optical axes of the laser and the FS-MOB is more difficult. To

address this issue, we have developed a novel optical beam-steering device to adjust the height of the optical axis. The beam-steering device consists of two 45° mirrors integrated with linear translation stages. Vertical adjustment of beam height can be achieved by in-plane actuators.<sup>44</sup> This is very desirable since the actuators moving in the vertical direction typically have small travel distances.<sup>45</sup>

#### 4. Conclusions

In summary, a new surface-micromachined free-space micro-optical bench (FS-MOB) has been proposed to integrate *free-space micro-optical systems* on a single chip. The FS-MOB can monolithically integrate micro-optical elements, micropositioners, and microactuators on the same chip using the same surface-micromachining processes. Pre-alignment of the optical systems can be performed during the design process. Out-of-plane micro-Fresnel lenses, diffractive optical elements, refractive microlenses, microgratings, tunable filters, free-space fiber optic switches have been successfully demonstrated. Integration of the optical elements with micropositioners (e.g., gratings on a rotational stage) as well as the incorporation of active optoelectronic devices using novel three-dimensional alignment structures have also been demonstrated. The FS-MOB technology enables us to build single-chip micro-optical systems by batch processing techniques, which can significantly reduce the size, weight, and cost of most optical systems. They have many applications in free-space optical interconnects, optical sensors, switches, data storage systems, and packaging of optoelectronic components.

#### Acknowledgments

This research is supported in part by DARPA, NCIPT, and the Packard Foundation. Part of the micromachined devices were fabricated by the DARPA-sponsored MUMPs fabrication services.

#### References

1. S. E. Miller, "Integrated optics: An introduction", *Bell Syst. Tech. J.* **48** (1969) 2059–2068.
2. T. L. Koch and U. Koren, "Semiconductor photonic integrated circuits", *IEEE J. Quantum Electron* **27** (1991) 641–653.
3. K. E. Petersen, "Silicon as a mechanical material", in *Proc. IEEE* **70** (1982) 420–457.
4. M. E. Motamedi, "Micro-opto-electro-mechanical systems", *Opt. Eng.* **33** (1994) 3505–3517.
5. K. E. Petersen, "Silicon torsional scanning mirror", *IBM J. Res. Develop.* **24** (1980) 631–637.
6. L. J. Hornbeck, "Deformable-mirror spatial light modulators", in *Proc. SPIE* **1150** (1990) 86–102.
7. L. J. Hornbeck, "Digital light processing and MEMS: Timely convergence for a bright future", *Proc. SPIE Symp. on Micromachining and microfabrication*, Austin, Tx., Oct. 1995.

8. O. Solgaard, F. S. A. Sandejas, and D. Bloom, "Deformable grating optical modulator", *Opt. Lett.* **17** (1992) 688–690.
9. M. T. Ching, R. A. Brennen, and R. M. White, "Microfabricated optical chopper", in *Proc. SPIE 1992* (1993) 40–46.
10. S. A. A. Yasseen, S. W. Smith, M. Mehregany, and F. L. Merat, "Diffraction grating scanners using polysilicon micromotors", in *Proc. IEEE Micro Electro Mechanical Systems*, Amsterdam, Netherland, 1995.
11. J. J. Yao and N. C. MacDonald, "A micromachined, single-crystal silicon tunable resonator", *J. Micromech. and Microeng.* **5** (1995) 257–264.
12. E. C. Vail, M. S. Wu, G. S. Li, L. Eng, and C. J. Chang-Hasnain, "GaAs micromachined widely tunable Fabry-Pérot filters", *Electron. Lett.* **31** (1995) 228–229.
13. T. R. Ohnstein, J. D. Zook, J. A. Cox, B. D. Speidrich, T. J. Wagener, H. Guckel, T. R. Christenson, J. Klein, T. Earles, and I. Glasgow, "Tunable IR filters using flexible metallic microstructures", in *Proc. 1995 IEEE Micro Electro Mechanical Systems*, Amsterdam, Netherland, Jan. 1995.
14. L. Y. Lin, J. L. Shen, S. S. Lee, M. C. Wu, and A. M. Sergent, "Tunable three-dimensional solid Fabry-Pérot Etalons fabricated by surface-micromachining", *IEEE Photon. Technol. Lett.* **8** (1996) 101–103.
15. A. T. T. D. Tran, Y. H. Lo, Z. H. Zhu, D. Haronian, and E. Mozdy, "Surface micromachined Fabry-Pérot tunable filter", *IEEE Photon. Technol. Lett.* **8** (1996) 393–395.
16. Y. Uenishi, M. Tsugai, and M. Mehregany, "Hybrid-integrated micromirror of laser-diode fabricated by (110) silicon micromachining", *Electron. Lett.* **31** (1995) 965–966.
17. M. S. Wu, E. C. Vail, G. S. Li, W. Yuen, and C. J. Chang-Hasnain, "Tunable micromachined vertical cavity surface-emitting laser", *Electron. Lett.* **31** (1995) 1671–1672.
18. M. C. Larson and J. S. Harris, "Wide and continuous wavelength tuning in a vertical-cavity surface-emitting laser using a micromachined deformable membrane mirror", *Appl. Phys. Lett.* **68** (1996) 891–893.
19. M. F. Dautartas, A. M. Benzoni, Y. C. Chen, G. E. Blonder, B. H. Johnson, C. R. Paola, E. Rice, and Y. H. Wong, "A silicon-based moving mirror optical switch", *J. Lightwave Technol.* **8** (1992) 1078–1085.
20. P. O. Haugsjaa, G. A. Duchene, J. F. Mehr, A. J. Negri, and M. J. Tabasky, "Progress towards low-cost silicon waferboard optical interconnects", in *Proc. 1994 IEEE Lasers and Electro-Optics Soc. Ann. Mtg.* Boston, MA, Oct. 1994, pp. 61–62.
21. L. S. Fan, Y. C. Tai, and R. S. Muller, "IC-processed electrostatic micromotors", *Sensors and Actuators* **20** (1989) 41–47.
22. R. T. Howe, R. S. Muller, K. J. Gabriel, and W. S. N. Trimmer, "Silicon micromechanics: Sensors and actuators on a chip", *IEEE Spectrum*, p. 20, July 1990.
23. A. P. Lee and A. P. Pisano, "Polysilicon angular microvibromotors", *J. Microelectromech. Syst.* **1** (1992) 70–76.
24. T. Akiyama and K. Shono, "Controlled stepwise motion in polysilicon microstructures", *J. Microelectromech. Sys.* **2** (1993) 106–110.
25. J. H. Comtois, V. M. Bright, and M. W. Phipps, "Thermal microactuators for surface-micromachining processes", in *Proc. SPIE 2642* (1995) 10–21.
26. K. S. J. Pister, M. W. Judy, S. R. Burgett, and R. S. Fearing, "Microfabricated hinges", *Sensors and Actuators A* **33** (1992) 249–256.
27. M. C. Wu, L. Y. Lin, and S. S. Lee, "Micromachined free-space integrated optics", in *Proc. SPIE 2291 Integrated Optics and Microstructures II*, San Diego, California, July 1994, pp. 40–51.
28. M. C. Wu, L. Y. Lin, S. S. Lee, and K. S. J. Pister, "Micromachined free-space integrated micro-optics", *Sensors and Actuators: A Physical* **50** (1995) 127–134.

29. L. Y. Lin, S. S. Lee, K. S. J. Pister, and M. C. Wu, "Three-dimensional micro-Fresnel optical elements fabricated by micromachining technique", *Electron. Lett.* **30** (1994) 448–449.
30. L. Y. Lin, S. S. Lee, K. S. J. Pister, and M. C. Wu, "Micro-machined three-dimensional micro-optics for integrated free-space optical system", *IEEE Photon. Technol. Lett.* **6** (1994) 1445–1447.
31. C. R. King, L. Y. Lin, and M. C. Wu, "Monolithically integrated refractive microlens standing perpendicular to the substrate", in *Proc. SPIE 2687* San Jose, CA, Jan. 1996, pp. 123–130.
32. S. S. Lee, L. Y. Lin, and M. C. Wu, "Surface-micromachined free-space micro-optical systems containing three-dimensional micro-gratings", *Appl. Phys. Lett.* **67** (1995) 2135–2137.
33. O. Solgaard, M. Daneman, N. C. Tien, A. Friedberger, R. S. Muller, and K. Y. Lau, "Optoelectronic packaging using silicon surface-micromachined aligned mirrors", *IEEE Photon. Technol. Lett.* **7** (1995) 41.
34. J. L. Shen, L. Y. Lin, S. S. Lee, M. C. Wu, and A. M. Sergent, "Surface-micromachined tunable three-dimensional solid Fabry-Pérot Etalons with dielectric coatings", *Electron. Lett.* **31** (1995) 2172–2173.
35. M. J. Daneman, O. Solgaard, N. C. Tien, K. Y. Lau, and R. S. Muller, "Laser-to-fiber coupling module using a micromachined alignment mirror", *IEEE Photon. Technol. Lett.* **8** (1996) 396–398.
36. D. S. Gunawan, K. S. J. Pister, and L. Y. Lin, "Micromachined coner cube reflectors as a communication link", *Sensors and Actuators A* **47** (1995) 580.
37. S. S. Lee, L. Y. Lin, and M. C. Wu, "Surface-micromachined free-space fiber optic switches", *Electron. Lett.* **31** (1995) 1481–1482.
38. L. Y. Lin, J. L. Shen, S. S. Lee, and M. C. Wu, "Realization of novel monolithic free-space optical disk pickup heads by surface micromachining", *Opt. Lett.* **21** (1996) 155–157.
39. M. H. Kiang, O. Solgaard, R. S. Muller, and K. Lau, "Surface-micromachined electrostatic-comb driven scanning micromirrors for barcode scanners", in *Proc. 1996 IEEE Workshop in Micro Electro Mechanical Systems*, San Diego, CA, Feb. 1996, pp. 192–197.
40. L. Y. Lin, S. S. Lee, K. S. J. Pister, and M. C. Wu, "Self-aligned hybrid integration of semiconductor lasers with micromachined micro-optics for optoelectronic packaging", *Appl. Phys. Lett.* **66** (1995) 2946–2948.
41. S. S. Lee, L. Y. Lin, K. S. J. Pister, M. C. Wu, H. C. Lee, and P. Grodzinski, "Passively aligned hybrid integration of  $8 \times 1$  micromachined micro-Fresnel lens arrays and  $8 \times 1$  vertical cavity surface-emitting laser arrays for free-space optical interconnect", *IEEE Photon. Technol. Lett.* **7** (1995) 1031–1033.
42. K. W. Markus and D. A. Koester, "Multi-User MEMS process (MUMPs) introduction and design rules", *MCNC Electronics Tech. Div. Research Triangle Park*, North Carolina, Oct. 1994.
43. K. Rastani, A. MARRAKCHI, S. F. Habiby, W. M. Hubbard, H. Gilchrist, and R. E. Nahory, "Binary phase Fresnel lenses for generation of two-dimensional beam arrays", *Appl. Opt.* **30** (1991) 1347–1354.
44. L. Y. Lin, S. S. Lee, and M. C. Wu, "45° out of plane beam steering optics for vertical alignment in free-space micro-optical bench", in *Proc. Conf. Lasers and Electron-Optics (CLEO)*, Paper CFC5, Anaheim, CA, June 1996.
45. A. Selvakumar, K. Najafi, W. H. Juan, and S. Peng, "Vertical comb array microactuators", *IEEE Workshop on Micro Electro Mechanical Systems*, Amsterdam, Netherlands, 1995, pp. 43–48.